Cancer associated fibroblasts and alectinib switch the evolutionary games that non-small cell lung cancer plays

Artem Kaznatcheev[1,2], Jeffrey Peacock[3], David Basanta[4], Andriy Marusyk[5], and Jacob G. Scott[2]

[1]Department of Computer Science, University of Oxford, Oxford, UK
[2]Department of Translational Hematology & Oncology Research, Cleveland Clinic, Cleveland, OH, USA
[3]Department of Radiation Oncology, Moffitt Cancer Center, Tampa, FL, USA
[4]Department of Integrated Mathematical Oncology, Moffitt Cancer Center, Tampa, FL, USA
[5]Department of Cancer Imaging and Metabolism, Moffitt Cancer Center, Tampa, FL, USA

August 21, 2017

Tumors are heterogeneous, evolving ecosystems [1, 2], composed of sub-populations of neoplastic cells that follow distinct strategies for survival and propagation [3]. The success of a strategy defining any single neoplastic sub-population is dependent on the distribution of other strategies, and on various components of the tumour microenvironment like cancer associated fibroblasts (CAFs) [4]. The rules mapping the population's strategy distribution to the fitness of individual strategies can be represented as an evolutionary game [5–12]. In four different environments, we measure the games between treatment naive (Alectinib therapy sensitive) cells and a derivative line in which resistance was previously evolved [13]. We find that the games are not only qualitatively different between different environments, but that targeted therapy and the presence of CAFs qualitatively switch the type of game being played. This provides the first empirical confirmation for the theoretical postulate of evolutionary game theory (EGT) in mathematical oncology that we can treat not just the player, but also the game. Although we concentrate on measuring games played by cancer cells, the measurement methodology we develop can be used to advance the study of games in other microscopic systems.

The EML4-ALK fusion, found in approximately 5% of NSCLC patients, leads to constitutive activation of oncogenic tyrosine kinase activity of ALK, therefore "driving" the disease. Inhibitors of tyrosine kinase activity of ALK (ALK - TKI) proved to be highly clinically efficacious, inducing tumor shrinkage and prolonging patient survival [14]. Unfortunately, virtually all of the tumors that respond to ALK TKIs eventually relapse [15] which is a typical outcome of other oncognic tyrosine kinases [16], resistance to ALK-TKI remains a major unresolved clinical challenge. Despite significant advances in deciphering molecular mechanisms of resistance [17], the evolutionary dynamics of the ALK TKI resistance remains poorly understood. The inability of TKI therapies to completely eliminate tumor cells has been shown to be at least partially attributable to microenvironmental protection [18]. CAFs are one of the main non-malignant components of tumor microenvironment and a major contributor to microenvironmental resistance, including cytokine mediated protection against ALK inhibitors [19]. To study these eco-evolutionary dynamics, we interrogated the competition between treatment naive H3122 cells and a derivative cell line in which we developed alectinib (a highly effective clinical ALK TKI) resistance by selection in progressively increasing concentrations of the drug [13]. Through these interrogations, we aimed to come to a quantitative understanding of how these dynamics were affected by clinically relevant concentrations of alectinib (0.5μM) in the presence or absence of CAFs.

Due to our interest in frequency-dependent biological interactions, we performed these experiments over a range of initial proportions of resistant and parental cells for each of the four environments. Other microscopic experimental systems in which frequency dependent fitness has been considered include, but are not limited to: E. coli [20, 21], yeast [22], bacterial symbionts of hydra [23], and pancreatic cancer [11], though none has been designed to measure evolutionary games directly. We used time lapse microscopy to follow the expansion of therapy resistant and parental cells, differentially labeled with stable expression of selectively neutral GFP and mCherry fluorescent proteins, respectively.

To establish baseline characteristics, we performed assays in monotypic cultures. From the time series data, we inferred the growth rate of both the parental and resistant cells for each of 6 replicates of each experimental condition, as seen in Figure 1A. As expected, alectinib inhibited growth rates of parental cells, whereas the growth rate of the resistant cells was not affected. And as previously reported [19], we observed stromal protection against ALK TKI: CAFs provided a more significant growth advantage in the presence of alectinib.

While the results of the monotypic culture matched expectations, we observed a number of non-intuitive nuances in our co-culture experiments. Figure 1B shows the resulting growth rates of each cell type in the co-culture experiments for all experimental (color, shape) and initial conditions (opacity is parental cell proportion). In the co-culture – unlike the monoculture – CAFs slightly improved the growth rates of the parental cells even in DMSO. More strikingly, even in the absence of drug, resistant cells tend to have a higher growth rate that parental cells. This is evident from most points being above the dotted diagonal line corresponding to equal

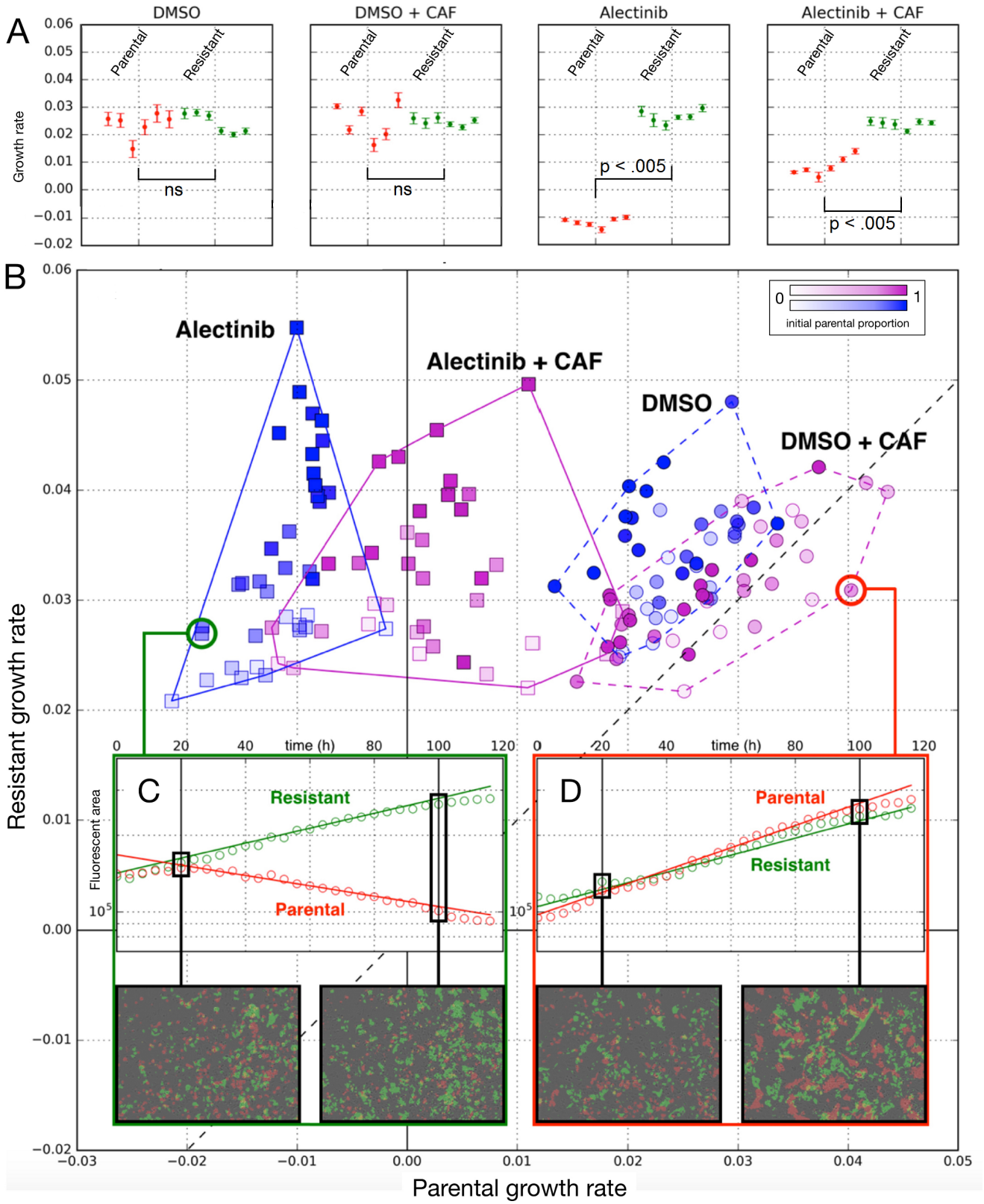

Figure 1: Coculture changes the fitness of cells in vitro. (a) Growth rates of the resistant and parental cells in indicated experimental conditions in monotypic cultures. Comparisons with Wilcoxon rank-sum. (b) Growth rates of resistant and parental cells for each well in four different conditions in coculture with varying seeding proportions of parental cells. See Figure 2 for growth rate confidence intervals. (c,d): indicated data points were generated by measuring red and green fluorescent area over time, and fitting an exponential growth model.

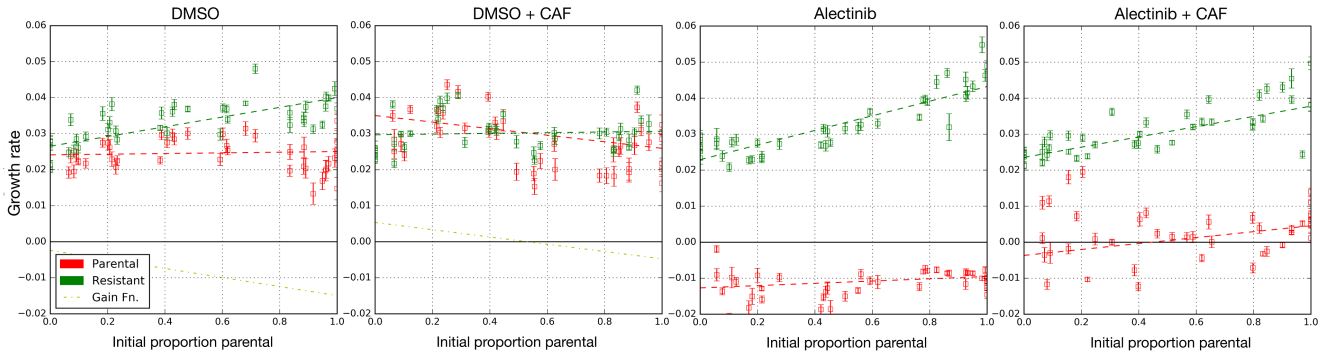

Figure 2: Fitness functions for competition of parental vs. resistant NSCLC. For each plot: growth rate with confidence intervals versus initial proportion of parental cells. Red data points are growth rates of parental cells, and green for resistant cells. Dotted lines represent the linear fitness function of best fit, and the yellow dotted line is the gain function for parental (see Figure 3a); fit error visualized in Figure 3b.

growth rate of the sub-populations ($y = x$). This is somewhat counter to standard considerations as while the emergence of therapeutic resistance is inevitable, it is broadly assumed that in the absence of treatment the resistant phenotype is neutral or even carries some inherent cost. For example, the experimental community assumes that the resistance granting mutation might have absolutely no effect in the absence of drug and the modeling community considers explicit costs like the up-regulating pumps to remove the drug, investing in other defensive strategies, or lowering growth rate by switching to sub-optimal growth pathways [3, 24]. In the presence of drug, resistance provides a relative benefit from increases survival or drug tolerance which – for modelers – offsets the cost. The higher fitness of resistant cells in our data throws in question this classic model of resistance, and is incompatible with a widely held assumption that resistance arises simply from selection of pre-existant sub-populations, which have been converted to resistance with a binary mutational switch [25].

Further, frequency dependence of both the parental and resistant cell growth rates is hinted at in Figure 1 where we see an increase in fitness of both cell types as the initial proportion of parental cells – represented by the opacity of each point – increases. This is shown more clearly in Figure 2. In all four conditions, we see that the growth rate of the resistant and parental cell lines depends linearly on the initial proportion of parental cells. In three of the conditions, the resistant cell growth rates increase with increased seeding proportion of parental cells, while the parental growth rates remain relatively constant (in the case of no CAFs) or slightly increasing (in the case of alectinib + CAFs). For example, in DMSO, this suggests that parental cells' fitness is independent of resistant cells: $w_P^{\text{DMSO}} = 0.025$. [1] However, resistant cells in monotypic culture have approximately the same fitness as parental cells (Figure 1a), but they benefit from the parental cells: $w_R^{\text{DMSO}} = 0.025 + 0.015p$ (where p is the proportion of parental cells). [2] This suggests commensalism between resistant and parental cells, i.e. resistant cells benefit from the interaction with the parental cells, without exerting positive or negative impact on them. The DMSO + CAF case differs from the other three in that we see a constant growth rate in resistant cells, but a linearly decreasing (in p) growth rate of parental cells: $w_P^{\text{DMSO + CAF}} = 0.025 + 0.01(1-p)$.[3] This could be interpreted as CAFs switching the direction of commensalism between parental and resistant cells.

The tools of evolutionary game theory are well suited for making sense of such frequency-dependent fitness. In measuring the game that describes this interaction, it is important to focus on the gain function (see [12, 26] for a theoretical perspective): the increase in growth rate that a hypothetical player would get in 'switching' from being parental to resistant with all other variables held constant. In other words, we need to look at how the difference between resistant and parental growth rates varies with initial proportion of parental cells. The relatively good fit of a linear dependence of growth rates on parental seeding proportion allows us to model the interaction as a matrix game – a well-studied class of evolutionary games (see model in Figure 3a). Note that this linearity is not guaranteed for arbitrary experimental systems. For example, the game between the two Betaproteobacteria *Curvibacter* sp. AEP1.3 and *Duganella* sp. C1.2 was described by a quadratic gain function [23].

Two strategy matrix games have a convenient representation in a two dimensional game-space and can produce all possible linear gain functions. More importantly, from a linear gain function, it is possible to infer the corresponding matrix game, up-to constant offsets on each column. Since the game type and resultant dynamics are invariant under constant offsets to the columns, this means we can infer the game played by the cancer cells (see the model in Figure 3a for details). We plot the inferred games in a game-space spanned by the theoretical fitness advantage a single resistant invader would have if introduced into a parental monotypic culture versus the fitness advantage of a parental invader in a resistant monotypic culture; as shown in Figure 3b. In this representation, there are four qualitatively different types of games corresponding to the four quadrants with an illustrative dynamic flow inset

[1] The actual line of best fit is $\hat{w}_P^{\text{DMSO}} = 0.025 - 0.001p$. This empirical fit has uncertainty, and w_P^{DMSO} is within the error-bars of $\hat{w}_P^{\text{DMSO}}$.

[2] The empirical line of best fit is $\hat{w}_R^{\text{DMSO}} = 0.027 + 0.013p$. But w_R^{DMSO} is within error of $\hat{w}_R^{\text{DMSO}}$.

[3] The empirical line of best fit is $\hat{w}_P^{\text{DMSO + CAF}} = 0.035 - 0.009p$. But $w_P^{\text{DMSO + CAF}}$ is within error of $\hat{w}_P^{\text{DMSO + CAF}}$.

$$
\begin{array}{c|cc} & P & R \\ \hline P & A & B \\ R & C & D \end{array}
\Rightarrow
\begin{cases}
\dfrac{d}{dt}N_P = N_P \overbrace{\left(A\dfrac{N_P}{N_P+N_R} + B\dfrac{N_R}{N_P+N_R}\right)}^{w_P\text{: parental growth rate}} \\[2ex]
\dfrac{d}{dt}N_R = N_R \underbrace{\left(C\dfrac{N_P}{N_P+N_R} + D\dfrac{N_R}{N_P+N_R}\right)}_{w_R\text{: resistant growth rate}}
\end{cases}
$$

$$
\Rightarrow \frac{dp}{dt} = p(1-p)\overbrace{\Big(\underbrace{(B-D)}_{\substack{\text{relative fitness of}\\ \text{parental invader}}}(1-p) - \underbrace{(C-A)}_{\substack{\text{relative fitness of}\\ \text{resistant invader}}}p\Big)}^{\text{gain function for } p}
$$

$$
\text{where } p = \frac{N_P}{N_P+N_R}.
$$

(a) Replicator dynamics for parental-resistant NSCLC.

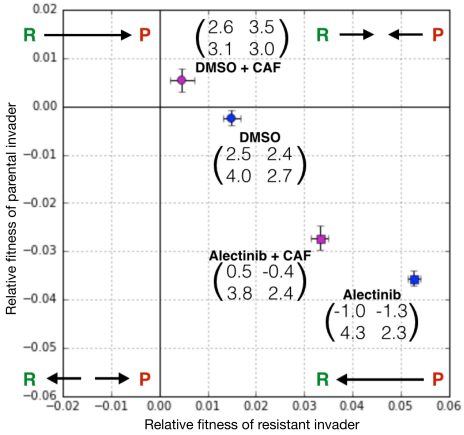

(b) Two dimensional game space.

Figure 3: Measured games. (a) Consider two strategies in a cancer cell co-culture: parental (P) and resistant (R). When P encounters P then each experience a fitness effect A; when P encounters R then$P$ experience fitness effect B and R fitness effect C; two Rs interaction experience fitness effects D. This is summarized in the matrix above, where the focal agent selects row and alter selects column; the matrix entry is then the fitness effect for the focal. This can be translated into a simple exponential growth model for the number of parental N_P and number of resistant N_R cells. The dynamics of the proportion of parental cells $p = \frac{N_P}{N_P+N_R}$ over time is described by the replicator equation (bottom). (b) We plot the four games measured in vitro. The games corresponding to our conditions are given as matrices (with entries multiplied by a factor of 100) by their label. The x-axis is the relative fitness of a resistant focal in a parental monotypic culture: $C - A$. The y-axis is the relative fitness of a parental focal in a resistant monotypic culture: $B - D$. This game space is divided into four possible dynamical regimes, one for each quadrant, represented as qualitative flow diagram between parental (P) and resistant (R) strategies (inset). Games measured in our experimental system are given as specific points with error bars based on goodness of fit of linear fitness functions in Figure 2.

in the corner of each quadrant. We can see that the game corresponding to DMSO + CAF – although quantitatively similar to DMSO – is of a qualitatively different type compared to all three of the other combinations.

Existing theoretical work considers treatment (or other environmental differences) as changes between qualitatively different game regimes [8–10, 12], with the goal not to directly target the cells, but instead perturb the game they are playing and allow evolution to drive unwanted cancer subclones to extinction through competition. This has been largely taken as a theoretical postulate. If we look at our emperical measurements for the untreated case with CAFs (upper-right quadrant Figure 3b) we see the Leader game. However, either treating with alectinib or eliminating CAFs through a stromal directed therapy, moves the game into the lower-right quadrant of Figure 3b, and the game becomes a Deadlock game. To our knowledge, neither of these games is considered in the prior theoretical EGT literature in oncology. This switch allows us to show that a popular theoretical construct of EGT in mathematical oncology – that treatment can qualitative change the type of game – has an experimental implementation.

A particularly important difference between Leader and Deadlock dynamics is the existence of an internal fixed point in Leader but not in Deadlock. We can see convergence towards this fixed point in the top-right panel (DMSO + CAF) of Figure 4, and no such convergence in the other three cases. Since the DMSO + CAF condition is our closest to an untreated patient, it has important consequences for latent resistance. Classical models of resistance assume a rare or *de novo* mutant taking over the population after the introduction of drug. In our experimental system, however, it is possible for negative frequency dependent selection to push the population towards a stable polyclonal tumour of resistant and sensitive cells before the introduction of drug. This allows for a much higher levels of pre-existing heterogeneity in resistance than predicted by the classical picture of costly drug resistance in the tumour prior to treatment. With this pre-existing heterogeneity, tumour resistance can emerge faster and more robustly; helping us to better understand why all patients eventually develop resistance to Alectinib.

Drug-sensitive (parental) and resistant cells interact not only with alectinib, but also with each other and microenvironmental factors like CAFs. We showed that the relative fitness advantage of resistant over parental cells – the gain function characterizing replicator dynamics – is a linear function of the initial proportion of sensitive cells. Surprisingly, resistant cells have an advantage over parental cells even in DMSO, throwing into question the common theoretical postulate that resistance comes at a cost that has to be offset by a benefit only present in drug. Measuring the gain function has enabled us to represent the inter-dependence between parental and resistant cells as a matrix game. Not only are these games quantitatively different among the four environmental conditions – see Figure 3b – but they are also of two qualitatively different types: a Leader game in the case of DMSO + CAF and Deadlock in the other three cases.

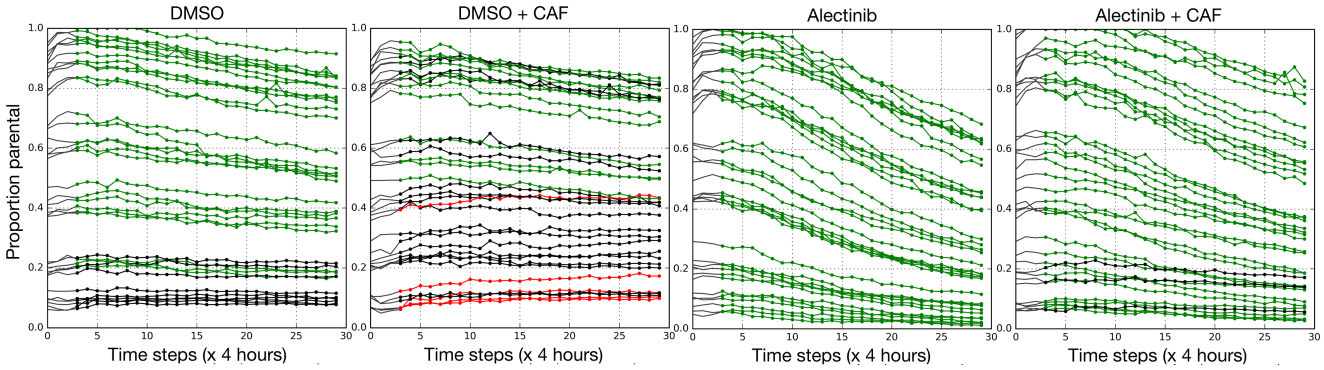

Figure 4: Proportion of parental cells versus time for competition of parental vs. resistant NSCLC. Each line corresponds to the time dynamics of a separate well. A line is coloured green if proportion of resistant cells increased from start to end; red if proportion of parental cells increased; black if statistically indistinguishable proportions at start and end.

This ability of treatment to qualitative change the type of game being played provides the first empirical demonstration of the principal: don't treat the player, treat the game. Our hope is that this empirical connection allows for potential translations of existing oncologic EGT literature to the clinic. Unfortunately, the Leader and Deadlock games are understudied in mathematical oncology, and we hope that our observation of them will motivate theorists to explore them in more detail. One difference between these game types is already clear: in the case of Leader there is a predicted negative frequency dependence selection toward a coexistence of parental and resistant cells – which we confirm for DMSO + CAF in Figure 4 – while for Deadlock there is selection towards a completely resistant tumour. Since the DMSO + CAF is the closest analog to a pre-treatment patient in our *in vitro* system, this suggests that there might be much higher levels of initial heterogeneity in drug resistance than prior theory would suggest. and throws into question the concept of rare pre-existent resistant clones. If this result holds *in vivo* and/or for other cancers it will help explain the ubiquity and speed of resistance that undermines our abilities to cure patients or control their disease. Building a catalog of the games cancers play – by adopting our methodology in other cancers, and other experimental contexts – can help resolve this and others questions, and allow for a new strategy in cancer therapy: treating the game.

Acknowledgements

JGS would like to acknowledge the NIH Loan Repayment program for their generous support of his research in general as well as Miles for Moffitt for generously supporting this work. We would also like to thank Mohamed Abazeed and Peter Jeavons for helpful discussions.

Methods

H3122 cell line was purchased from ATCC (Manassas, Virginia). Identity of cell lines was confirmed by short tandem repeats (STR) analysis, performed at Moffitt Cancer Center Molecular Genetics core facility. Primary lung cancer associated fibroblasts were obtained from S. Antonia lab (Moffitt Cancer Center). The cells were isolated as previously described [27] and expanded for 3-10 passages prior to the experiments. All human tissue was collected using protocols approved by the USF Institutional Review Board. Alectinib resistant derivative cell line was obtained through escalating inhibitor concentration protocol, as described in Dhawan *et al.* [13]. Stable GFP and mCherry expressing derivative cell H3122 cell lines were obtained through lentiviral transduction with pLVX-AcGFP (Clontech) and mCherry (obtained from K. Mitsiades, DFCI) respectively. Both H3122 cells and CAFs were cultured in RPMI media (Gibco brand from Thermo Scientific), supplemented with 10% FBS, (purchased from Serum Source, Charlotte, NC). Regular tests for mycoplasma contamination were performed with MycoScope PCR based kit from GenLantis, San Diego, CA.

The cells were harvested upon reaching 70% confluence and counted using Countess II automatic cell counter (Invitrogen). For the determination of competitive growth rates, 2,000 H3122 cells were seeded with or without 500 CAF cells in 50 ul RPMI media per well into 384 well plates (Corning, catalogue #7200655), with different proportions of differentially labelled parental and alectinib resistant variants. 20 hours after seeding, Alectinib – that was purchased from ChemieTek (Indianapolis, IN) – or DMSO vehicle control, diluted in 20 ul RPMI were added to each well, to achieve final Alectinib concentration of 500 nM/l. Time lapse microscopy measurements were performed every 4 hours in white light, as well as green and red fluorescent channels using Incucyte Zoom system from Essen Bioscience.

Units of size for populations was fluorescent area, measured from timelapse images via python code using the OpenCV package. We cleaned images by renormalizing them (GFP and mCherry intensities vary over different orders of magnitude), removing vignetting with CLAHE, and thresholding to identify fluorescent regions. We eliminate salt-and-pepper noise from the thresholded images with the opening morphological transform. The resultant area is then taken as measure of population size for the purposes of computing fitnesses. In order to minimize the impact of growth inhibition by confluency, we analyzed the competitive dynamics during the first

5 days of culture, when the cell population was expanding exponentially. We use growth rate as our measure of fitness. We learn growth rate along with a confidence interval from the time-series of population size in each well using the Theil-Sen estimator. The above is summarized in 1c,d.

Since raw population sizes have different units (GFP Fluorescent Area (GFA) vs mCherry Fluorescent Area (CFA)), we converted them to common cell-number units by learning the linear transform that scales GFA and CFA into cell-number. In Figure 2, to measure the fitness functions we plotted in fitness of each cell-type in each well vs seeding proportion (p) of parental cells – computed from the first time-point. We estimated the line of best-fit and error on parameters for this data using least-squares. The $p = 0$ and $p = 1$ intercepts of the fitness functions serve as the entries of the game matrices in Figure 3b. The game point are calculated from the matrices, and the error is propagated from the error estimates on fitness function's parameters.

Code and data are available on request.

References

1. Merlo, L. M., Pepper, J. W., Reid, B. J. & Maley, C. C. Cancer as an evolutionary and ecological process. *Nature Reviews Cancer* **6,** 924–935 (2006).
2. Heppner, G. H. Tumor heterogeneity. *Cancer Research* **44,** 2259–2265 (1984).
3. Ibrahim-Hashim, A. *et al.* Defining cancer subpopulations by adaptive strategies rather than molecular properties provides novel insights into intratumoral evolution. *Cancer Research,* 2844 (2017).
4. Scott, J. & Marusyk, A. Somatic clonal evolution: A selection-centric perspective. *Biochimica et Biophysica Acta: Reviews on Cancer* (2017).
5. Maynard Smith, J & Price, G. R. The Logic of Animal Conflict. *Nature* **246,** 15 (1973).
6. Tomlinson, I. P. & Bodmer, W. F. Modelling the consequences of interactions between tumour cells. *British Journal of Cancer* **75,** 157–160 (1997).
7. Tomlinson, I. P. Game-theory models of interactions between tumour cells. *European Journal of Cancer* **33,** 1495–1500 (1997).
8. Basanta, D. *et al.* Investigating prostate cancer tumour–stroma interactions: clinical and biological insights from an evolutionary game. *British Journal of Cancer* **106,** 174–181 (2012).
9. Archetti, M. Evolutionary game theory of growth factor production: implications for tumour heterogeneity and resistance to therapies. *British Journal of Cancer* **109,** 1056–1062 (2013).
10. Kaznatcheev, A., Scott, J. G. & Basanta, D. Edge effects in game-theoretic dynamics of spatially structured tumours. *Journal of The Royal Society Interface* **12,** 20150154 (2015).
11. Archetti, M., Ferraro, D. A. & Christofori, G. Heterogeneity for IGF-II production maintained by public goods dynamics in neuroendocrine pancreatic cancer. *Proceedings of the National Academy of Sciences* **112,** 1833–1838 (2015).
12. Kaznatcheev, A., Vander Velde, R., Scott, J. G. & Basanta, D. Cancer treatment scheduling and dynamic heterogeneity in social dilemmas of tumour acidity and vasculature. *British Journal of Cancer* (2017).
13. Dhawan, A. *et al.* Collateral sensitivity networks reveal evolutionary instability and novel treatment strategies in ALK mutated non-small cell lung cancer. *Scientific Reports* **7** (2017).
14. Shaw, A. T. *et al.* Crizotinib versus chemotherapy in advanced ALK-positive lung cancer. *New England Journal of Medicine* **368,** 2385–2394 (2013).
15. Shaw, A. T. & Engelman, J. A. ALK in lung cancer: past, present, and future. *Journal of Clinical Oncology* **31,** 1105–1111 (2013).
16. Gillies, R. J., Verduzco, D. & Gatenby, R. A. Evolutionary dynamics of carcinogenesis and why targeted therapy does not work. *Nature Reviews Cancer* **12,** 487–493 (2012).
17. Katayama, R., Lovly, C. M. & Shaw, A. T. Therapeutic targeting of anaplastic lymphoma kinase in lung cancer: a paradigm for precision cancer medicine. *Clinical Cancer Research* **21,** 2227–2235 (10 2015).
18. Marusyk, A. *et al.* Spatial proximity to fibroblasts impacts molecular features and therapeutic sensitivity of breast cancer cells influencing clinical outcomes. *Cancer Research* **76,** 6495–6506 (2016).
19. Yamada, T. *et al.* Paracrine receptor activation by microenvironment triggers bypass survival signals and ALK inhibitor resistance in EML4-ALK lung cancer cells. *Clinical Cancer Research* **18,** 3592–3602 (2012).
20. Kerr, B., Riley, M. A., Feldman, M. W. & Bohannan, B. J. Local dispersal promotes biodiversity in a real-life game of rock–paper–scissors. *Nature* **418,** 171–174 (2002).
21. Maddamsetti, R., Lenski, R. E. & Barrick, J. E. Adaptation, clonal interference, and frequency-dependent interactions in a long-term evolution experiment with Escherichia coli. *Genetics* **200,** 619–631 (2015).
22. Gore, J., Youk, H. & Van Oudenaarden, A. Snowdrift game dynamics and facultative cheating in yeast. *Nature* **459,** 253–256 (2009).
23. Li, X.-Y. *et al.* Which games are growing bacterial populations playing? *Journal of The Royal Society Interface* **12,** 20150121 (2015).
24. Anderson, A. R., Weaver, A. M., Cummings, P. T. & Quaranta, V. Tumor morphology and phenotypic evolution driven by selective pressure from the microenvironment. *Cell* **127,** 905–915 (2006).

25. Diaz Jr, L. A. *et al.* The molecular evolution of acquired resistance to targeted EGFR blockade in colorectal cancers. *Nature* **486,** 537 (2012).

26. Peña, J., Lehmann, L. & Nöldeke, G. Gains from switching and evolutionary stability in multi-player matrix games. *Journal of Theoretical Biology* **346,** 23–33 (2014).

27. Mediavilla-Varela, M., Boateng, K., Noyes, D. & Antonia, S. J. The anti-fibrotic agent pirfenidone synergizes with cisplatin in killing tumor cells and cancer-associated fibroblasts. *BMC Cancer* **16,** 176 (2016).